Sign Reversal of the Mn-O Bond Compressibility in $La_{1.2}Sr_{1.8}Mn_2O_7$ below T_C: Exchange Striction in the Ferromagnetic State

D. N. Argyriou,[1,*] J. F. Mitchell,[2] J. B. Goodenough,[3] O. Chmaissem,[1] S. Short,[2] and J. D. Jorgensen[2]
[1]*Science and Technology Center for Superconductivity, Argonne National Laboratory, Argonne, Illinois 60439*
[2]*Materials Science Division, Argonne National Laboratory, Argonne, Illinois 60439*
[3]*Center for Material Science and Engineering, ECT 9.102, University of Texas at Austin, Austin, Texas 78712-1063*
(Received 28 August 1996)

The crystal structure of the layered perovskite $La_{1.2}Sr_{1.8}Mn_2O_7$ has been studied under hydrostatic pressure up to ~6 kbar, in the paramagnetic and ferromagnetic states, with neutron powder diffraction. The compressibility of the Mn-O apical bonds in the double layer of MnO_6 octahedra changes sign from the paramagnetic insulator (PI) to the ferromagnetic metal (FM) state; in the FM state the Mn-O-Mn linkage between MnO_2 planes expands under applied pressure, whereas they contract in the PI state. This counterintuitive behavior is interpreted in terms of *exchange striction*, which reflects the competition between super and double exchange. An increase of the Mn moment with applied pressure in the FM state is consistent with a positive dT_C/dP, as well as a cant angle θ_0 between the magnetizations of neighboring MnO_2 sheets that decreases with pressure. [S0031-9007(97)02513-1]

PACS numbers: 75.80.+q, 75.25.+z

The physical properties of transition metal oxides are particularly sensitive to pressure where an increase in the overlap between oxygen-2p and cation-d orbitals induces a transition from localized (or strongly correlated) to itinerant electronic behavior, as found in the perovskite $PrNiO_3$ [1] and V_2O_3 [2]. Pressure affects magnetic properties where orbital degeneracies can lead to orbital ordering, as is illustrated by $LaVO_3$ [3]. In mixed valent systems such as in the double exchange ferromagnet $La_{1-x}Sr_xMnO_3$, both electronic and ferromagnetic transitions are coupled, and pressure increases the Curie temperature T_C [4,5]. This is in sharp contrast to other itinerant perovskite systems (e.g., $SrRuO_3$) where application of pressure generally leads to a suppression of T_C [6,7].

Recently, Moritomo *et al.* [8] have reported that the layered Ruddlesden-Popper compound $La_{1.2}Sr_{1.8}Mn_2O_7$ is a ferromagnetic metal (FM) below $T_C \sim 120$ K and a paramagnetic insulator (PI) above this temperature. They attribute the coupled electronic and magnetic transitions at T_C to a double exchange coupling in Mn-O-Mn linkages. Application of magnetic field on this compound leads to enhanced magnetoresistance (MR) (~20 000% at 129 K in 7 T, ~200% at 300 K in 0.3 T) with respect to a similarly doped perovskite material ($La_{0.825}Sr_{0.175}MnO_3$, ~200% in 7 T) [9]. In this paper we report the crystal structure of the layered, perovskite related compound $La_{1.2}Sr_{1.8}Mn_2O_7$ under hydrostatic pressure up to ~6 kbar, in both the PI and FM states. We demonstrate that of the two apical Mn-O bonds along the c axis, one expands with pressure while the other contracts. Remarkably, the compressibilities of both of these bonds change sign on traversing T_C. We argue that this unusual finding is a manifestation of *exchange striction* and predict that the compound is a canted-spin ferromagnet. This finding dramatically demonstrates how metal-oxygen bond strengths are modulated by metal-oxygen-metal interactions. Furthermore, it is an unusual example of an expansion of individual metal-oxygen bonds along an axis that shows a normal decrease with pressure.

Crystals of $La_{1.2}Sr_{1.8}Mn_2O_7$ were melt grown in flowing 20% O_2 (balance Ar) in a floating zone optical image furnace (NEC SC-M15HD). The sample exhibits a transition from a paramagnetic insulator to a ferromagnetic metal at 120 K, in good agreement with the report of Moritomo *et al.* [8]. Further details on the growth and characterization of this sample can be found elsewhere [10].

Time-of-flight neutron powder diffraction data were collected on the Special Environment Powder Diffractometer (SEPD) at Argonne's Intense Pulsed Neutron Source (IPNS) with the sample in a helium gas pressure cell [11]. Diffraction data were obtained for a series of pressures up to 6.5 kbar at 300, and 200 K in the paramagnetic state and 100 K in the ferromagnetic state.

Neutron diffraction patterns of $La_{1.2}Sr_{1.8}Mn_2O_7$ were consistent with a tetragonal cell, space group $I4/mmm$ at all pressures and temperatures. Powder diffraction patterns were analyzed with the Rietveld method and the program GSAS [12]. For data measured at 100 K additional magnetic scattering was consistent with previous ambient pressure observations that the Mn moment lies within the a-b plane in $La_{1.2}Sr_{1.8}Mn_2O_7$ [10]. Results of the Rietveld analysis for data measured at 300 and 100 K as a function of pressure are given in Table I. The crystal structure of $La_{1.2}Sr_{1.8}Mn_2O_7$ (Fig. 1) consists of double perovskite layers, each layer made up of a two dimensional network of MnO_6 octahedra. The La,Sr atoms are found between octahedra. Alternate perovskite bi-layers along the c axis are misaligned with respect to each other, as shown in Fig. 1.

A linear fit to refined lattice parameters as a function of pressure measured at 300, 200, and 100 K was used to compute the compressibility of $La_{1.2}Sr_{1.8}Mn_2O_7$ at these

 0031-9007/97/78(8)/1568(4)$10.00

TABLE I. Structural parameters for $La_{1.2}Sr_{1.8}Mn_2O_7$ at (a) 300 and (b) 100 K over the pressure range 0 to ~6.5 kbar. The space group used in the analysis of diffraction data was $I4/mmm$. In this structure the Mn is placed at $(0,0,z)$, La/Sr(1) at $(0,0,1/2)$, La/Sr(2) at $(0,0,z)$, O(1) at $(0,0,0)$, O(2) at $(0,0,z)$, and O(3) at $(0,1/2,0)$. The Mn-moment μ_{ab} at 100 K is given as μ_B/Mn.

T = 300 K		0.08 kbar	1.54 kbar	3.12 kbar	4.62 kbar	6.21 kbar
a (Å)		3.87197(5)	3.87044(5)	3.86893(5)	3.86737(5)	3.86598(5)
c (Å)		20.1083(5)	20.1043(5)	20.0981(5)	20.0937(5)	20.0888(5)
Mn	z	0.0968(2)	0.0968(2)	0.0966(2)	0.0965(2)	0.0966(2)
La/Sr(2)	z	0.3173(1)	0.3176(1)	0.3175(1)	0.3176(1)	0.3175(1)
O(2)	z	0.1957(2)	0.1961(2)	0.1963(1)	0.1962(1)	0.1959(2)
O(3)	z	0.0952(1)	0.0950(1)	0.0950(1)	0.0951(1)	0.0947(1)
T = 100 K		0.48 kbar	1.52 kbar	3.10 kbar	4.85 kbar	6.3 kbar
a (Å)		3.86706(5)	3.86602(5)	3.8649(5)	3.86305(5)	3.86124(5)
c (Å)		20.0475(5)	20.0463(5)	20.0423(5)	20.0366(5)	20.0326(5)
Mn	z	0.0966(2)	0.0967(2)	0.0968(3)	0.0970(3)	0.0971(3)
	μ_{ab}	2.51(7)	2.61(6)	2.68(6)	2.74(8)	2.80(6)
La/Sr(2)	z	0.3175(1)	0.3177(1)	0.3174(1)	0.3174(1)	0.3175(1)
O(2)	z	0.1960(2)	0.1961(2)	0.1959(2)	0.1958(2)	0.1958(2)
O(3)	z	0.0951(1)	0.0952(1)	0.0951(1)	0.0949(1)	0.0949(1)

temperatures [shown in Fig. 2(a)]. The a-axis compressibilities remain almost constant with temperature, while the c-axis compressibility becomes more positive (less compressible) with decreasing temperature. The combination of the a- and c-axis compressibility thus results in a volume compressibility that increases slightly with decreasing temperature [Fig. 2(b)]. The a-axis compressibility is accounted for wholly by the reduction of the Mn-O(3) bond length (−0.15% over 6 kbars) [Figs. 3(c) and 3(f)] for all temperatures examined; the Mn-O(3)-Mn bond angle remains unchanged within experimental error at 178.6(4)°, indicating no additional buckling of MnO_6 octahedra occurs with applied pressure. This is in contrast to other perovskite materials [13,14], where application

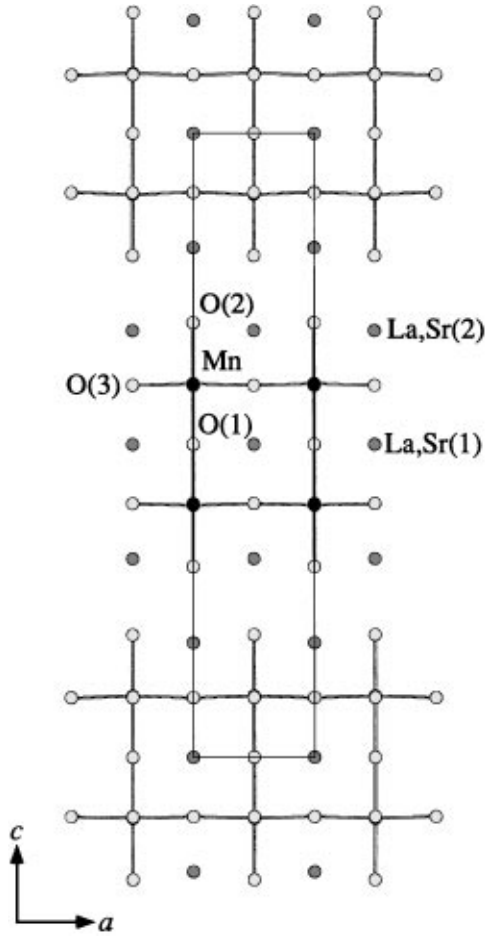

FIG. 1. The crystal structure of $La_{1.2}Sr_{1.8}Mn_2O_7$ projected along [010]. The unit cell is shown with a solid line.

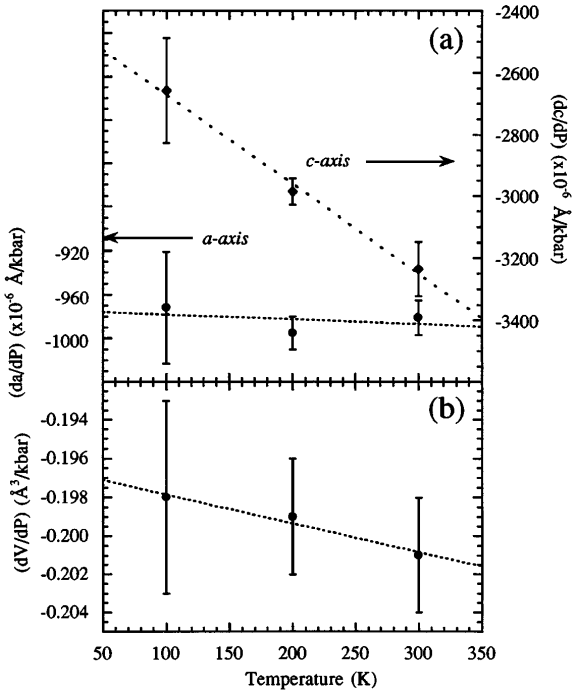

FIG. 2. The compressibilities of the a and c axis [upper panel (a)] and unit cell volume [lower panel (b)] vs. temperature.

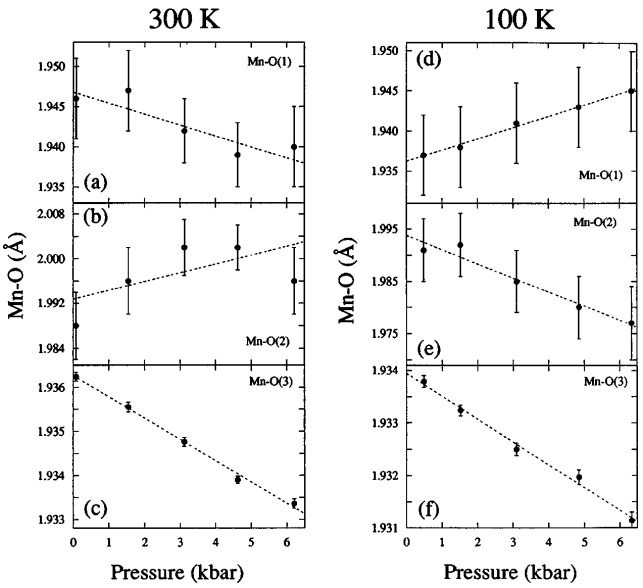

FIG. 3. The variation of Mn-O bond lengths in $La_{1.2}Sr_{1.8}Mn_2O_7$ with pressure at 300 K (a)–(c) and 100 K (d)–(f). Lines are weighted least-squares fits to the data.

of pressure results primarily in a tilting of the MnO_6 octahedra, rather than changes of the Mn-O bond lengths.

Although the c-axis compressibility changes linearly with temperature, Fig. 2, investigation of the compressibilities of the individual c-axis Mn-O bonds reveals two remarkable findings: (1) The pressure variations of distinguishable Mn-O(1) and Mn-O(2) bond lengths have opposite signs, and (2) the signs of these variations are opposite in the PI regime at 300 K, Figs. 3(a) and 3(b), to what they are in the FM state at 100 K, Figs. 3(d) and 3(e). The compressibilities of the individual Mn-O apical bonds are not in proportion to the overall c-axis compressibility [Fig. 2(a)], reflecting that the remainder of the lattice compensates for the compressibility of the perovskite double layer. That the O(1) and O(2) oxygen atoms share the same Mn $d_{3z^2-r^2}$ orbital while exhibiting opposite Mn-O compressibilities forces consideration of the Mn-O(1)-Mn interactions in contrast to the Mn-O(2)-La,Sr interactions.

The response of the individual Mn-O lengths to applied pressure in the PI and FM states reflects a change in the c-axis Mn-O-Mn interactions with the degree of ferromagnetic alignment of pairs of ferromagnetic MnO_2 sheets. The observed compressibilities are consistent with a magnetic structure in which the ferromagnetic MnO_2 sheets have magnetizations canted with respect to one another. To understand this model, two contributions to the c-axis Mn-O-Mn interactions need to be considered: the antiferromagnetic t^3-p_π-t^3 π-bonding component between half-filled t_{2g} orbitals of the high-spin Mn^{3+} or Mn^{4+} configurations and the ferromagnetic e^1-p_σ-e^0 component that dominates the σ-bonding interactions via electrons in the twofold-degenerate states of e_g-orbital parentage [15]. Both interactions involve a charge transfer that preserves the spin angular momentum. The t^3 configurations remain localized, so transfer of a t electron to create a t^4 configuration at a neighboring Mn atom requires an energy U_π and is constrained by the Pauli exclusion principle to have a component of the transferred electron spin antiparallel to the spin of the t^3 configuration at the acceptor Mn atom. This antiferromagnetic t^3-p_π-t^3 superexchange interaction is described by second-order perturbation theory; it gives a stabilization energy, $\varepsilon_t^s \sim -b_\pi^2 \sin^2(\theta/2)/U_\pi \sim b_\pi^2 \cos\theta/U_\pi$ where b_π is the spin-independent transfer-energy matrix element and θ is the angle between spins at neighboring Mn atoms along the c axis. A $\theta = \pi$ gives an attractive Mn-O-Mn interaction; a $\theta = 0$ gives a repulsive interaction.

The e^1-p_σ-e^0 interaction, on the other hand, involves transfer of an e electron to an empty e orbital; this transfer is not constrained by the Pauli exclusion principle, but a strong ferromagnetic intra-atomic exchange favors transfer to an acceptor having its spin ferromagnetically aligned with respect to that of the transferred electron. This ferromagnetic e^1-p_σ-e^0 interaction is stronger than the t^3-p_π-t^3 interaction whether the charge transfer is virtual (superexchange) or real (double-exchange). A real charge transfer is described by first-order theory, so it gives a stabilization $\varepsilon_\sigma^D \sim -b_\sigma \cos\theta/2$. In the FM state, the charge transfer between and within MnO_2 planes is real, and optimization of θ for the sum of the superexchange and double-exchange components gives a cant angle θ_0 if $\cos(\theta_0/2) \sim b_\sigma U_\pi/b_\pi^2 < 1$. A $\theta_0 = 0$ is stabilized below T_C *within* ferromagnetic MnO_2 planes, but the compressibility data imply a $\cos(\theta_0/2) < 1$ for the magnetic coupling *between* planes. Since b_σ contains a larger Mn-O overlap integral than b_π, pressure increases $\cos(\theta_0/2)$, thereby reducing the angle θ_0 and increasing the t^3-p_π-t^3 spin-spin repulsion between MnO_2 planes. A change in lattice parameters induced by changes in bonding as a result of magnetic order represents an *exchange striction;* a phenomenon common to magnetic oxides [15,16].

In $La_{1.2}Sr_{1.8}Mn_2O_7$, each Mn atom sees a Mn-O-Mn interaction on only one side along the c axis; the Mn-O-(La,Sr) interaction contains a Mn-O bond length that is free to adjust to that on the Mn-O-Mn side so as to retain the mean Mn-O bond length characteristic of the valence-bond sum, which is why the c-axis Mn-O bonds on opposite sides of a Mn atom vary reciprocally with temperature [10] and pressure. In the absence of magnetic order in the PI state, there is no spin-spin repulsion, and pressure increases the overlap integrals in both b_π and b_σ to give a normal reduction of the equilibrium Mn-O bond lengths within and between the MnO_2 sheets. This behavior is clearly seen for the Mn-O(1) and Mn-O(3) bonds at 300 K, Fig. 3. The Mn-O(2) bond length behaves differently because it is not part of the Mn-O-Mn linkage; see Fig. 1. It responds to the Mn-O(1) and Mn-O(3) bond-length changes so as to conserve the mean equilibrium bond-length sum for the Mn valences. We have omitted from this qualitative

discussion the influence of any redistribution of electrons between $d_{x^2-y^2}$ and $d_{3z^2-r^2}$ orbitals with pressure, as such a redistribution would not contribute to a sign reversal of the Mn-O(1) and Mn-O(2) compressibilities on crossing T_C.

In the absence of magnetic superlattice reflections, the neutron powder diffraction data are consistent with the type-A canted spin ferromagnetic model proposed. They indicate a ferromagnetic coupling within MnO_2 basal planes below T_C. Analysis of the diffraction data using models with a z component of the spin parallel to the c axis consistently produce values of $\mu_z = 0$ at all pressures examined. Because of the tetragonal symmetry of the lattice, single-crystal neutron-diffraction studies are needed to confirm whether there is the predicted cant angle in the a-b planes between spins of neighboring MnO_2 planes. However, an observed increase in the Mn moment from $2.5\mu_B$ to $2.8\mu_B$ over 6 kbar of pressure is consistent with the predicted decrease of cant angle θ_0 and a positive dT_C/dP for this compound.

In conclusion, the surprising reversal in the sign of the Mn-O(1) bond compressibility on passing from the PI to the FM state can be interpreted as a manifestation of exchange striction; a cant angle θ_0 between the magnetizations of the pairs of MnO_2 sheets within a perovskite layer is predicted for this layered manganite. The reciprocal response to temperature and pressure of the c-axis Mn-O(1) and Mn-O(2) bond lengths reflects the asymmetric c-axis bonding at a Mn atom; the Mn-O(2) bonds are free to adjust their length so as to retain the equilibrium bond-length sum for the Mn valences.

This work was supported by the U.S. Department of Energy, Basic Energy Sciences–Materials Sciences, and ER-LTT, under Contract No. W-31-109-ENG-38 (JFM, JDJ, SS) and by the NSF Office of Science and Technology Centers under DMR-91-20000 (DNA, OC). J. B. G. thanks the NSF and the Robert A. Welch Foundation, Houston, TX, for financial support.

*Present address: Los Alamos Neutron Science Center, MS 4805, Los Alamos National Laboratory, Los Alamos, New Mexico 87545

[1] P. L. Canfield, J. D. Thompson, S.-W. Cheong, and L. W. Rupp, Phys. Rev. B **47**, 12 357 (1993).
[2] X. Obradors, L. M. Paulius, M. B. Maple, J. B. Torrance, A. I. Nazzal, I. Fontcuberta, and X. Granados, Phys. Rev. B **47**, 12 353 (1993).
[3] H. C. Nguyen and J. B. Goodenough, Phys. Rev. B **52**, 324 (1995).
[4] Y. Moritomo, A. Asamitsu, and Y. Tokura, Phys. Rev. B **51**, 16 491 (1995).
[5] W. Archibald, J.-S. Zhou, and J. B. Goodenough, Phys. Rev. B **53**, 14 445 (1996).
[6] N. Menyuk, J. A. Kafalas, K. Dwight, and J. B. Goodenough, J. Appl. Phys. **40**, 1324 (1969).
[7] M. Shikano, T. Huang, Y. Inaguma, M. Itho, and T. Nakamura, Solid State Commun. **90**, 115 (1994).
[8] Y. Moritomo, A. Asamitsu, H. Kuwahara, and Y. Tokura, Nature (London) **380**, 141 (1996).
[9] A. Urushibara, Y. Moritomo, T. Arima, A. Asamitsu, G. Kido, and Y. Tokura, Phys. Rev. B **51**, 14 103 (1995).
[10] J. F. Mitchell, D. N. Argyriou, J. D. Jorgensen, D. G. Hinks, C. D. Potter, and S. D. Bader, Phys. Rev. B **55**, 63 (1997).
[11] J. D. Jorgensen, S. Pei, P. Lightfoot, D. G. Hinks, B. W. Veal, B. Dabrowski, A. P. Paulikas, and R. Kleb, Physica (Amsterdam) **171C**, 93 (1990).
[12] A. C. Larson and R. B. von Dreele, General Structure Analysis System, University of California (1985–1990).
[13] Y. Zhao, D. J. Weidner, J. B. Parise, and D. E. Cox, Phys. Earth Planet. Inter. **76**, 17 (1993).
[14] J.-E. Jorgensen, J. D. Jorgensen, B. Batlogg, J. P. Remeika, and J. D. Axe, Phys. Rev. B **33**, 4793 (1986).
[15] J. B. Goodenough, in *Progress in Solid State Chemistry*, edited by H. Reiss (Pergamon Press, Oxford, 1971), p. 145.
[16] J. B. Goodenough, *Magnetism and the Chemical Bond* (John Wiley & Sons, New York, 1963).